Journal of Structural Biology 179 (2012) 68–75

Contents lists available at SciVerse ScienceDirect

Journal of Structural Biology

journal homepage: www.elsevier.com/locate/yjsbi

Spotiton: A prototype for an integrated inkjet dispense and vitrification system for cryo-TEM

Tilak Jain *, Patrick Sheehan, John Crum, Bridget Carragher, Clinton S. Potter

The National Resource for Automated Molecular Microscopy, Department of Cell Biology, The Scripps Research Institute, 10550 North Torrey Pines Road, La Jolla, CA 92037, United States

ARTICLE INFO

Article history:
Received 17 February 2012
Received in revised form 19 April 2012
Accepted 25 April 2012
Available online 5 May 2012

Keywords:
Cryo electron microscopy
Cryo-TEM
Vitrification
Single particle EM

ABSTRACT

Over the last three decades, Cryo-TEM has developed into a powerful technique for high-resolution imaging of biological macromolecules in their native vitrified state. However, the method for vitrifying specimens onto EM grids is essentially unchanged – application of ~3 μL sample to a grid, followed by blotting and rapid plunge freezing into liquid ethane. Several trials are often required to obtain suitable thin (few hundred nanometers or less) vitrified layers amenable for cryo-TEM imaging, which results in waste of precious sample and resources. While commercially available instruments provide some level of automation to control the vitrification process in an effort to increase quality and reproducibility, obtaining satisfactory vitrified specimens remains a bottleneck in the Cryo-TEM pipeline. We describe here a completely novel method for EM specimen preparation based on small volume (picoliter to nanoliter) dispensing using inkjet technology. A first prototype system (Spotiton v0.5) demonstrates feasibility of this new approach for specimen vitrification. A piezo-electric inkjet dispenser is integrated with optical real-time cameras (100 Hz frame rate) to analyze picoliter to nanoliter droplet profiles in-flight and spreading dynamics on the grid, and thus provides a method to optimize timing of the process. Using TEM imaging and biochemical assays we demonstrate that the piezo-electric inkjet mechanism does not disrupt the structural or functional integrity of macromolecules. These preliminary studies provide insight into the factors and components that will need further development to enable a robust and repeatable technique for specimen vitrification using this novel approach.

1. Introduction

Over thirty years ago, Dubochet and colleagues (Dubochet and McDowall, 1981; Lepault et al., 1983) first demonstrated that biological specimens in their native hydrated state could be embedded in vitrified buffer and imaged in the transmission electron microscope (TEM) without loss of structural preservation. This paved the way for the development of cryo-TEM as a field (reviewed in (Dobro et al., 2010)) and the technique has been used to study a vast array of structures over the past three decades. During this period, there have been major technical advances in instrumentation, image processing and analysis algorithms used to extract three-dimensional structures from noisy and low contrast projection images (Jensen, 2010a,b,c). However, specimen preparation has essentially remained unchanged since first described in 1981 (Dubochet and McDowall, 1981); the typical protocol comprised of pipetting a volume (~3 μL) of sample onto the surface of a carbon film supported on a copper mesh grid, then blotting the sample to a thin layer by applying filter paper to one or both sides of the grid, followed by quickly plunging into liquid ethane (Fig. 1A). A variety of devices have been developed to optimize this method, including both home-made guillotine plungers and more automated commercial devices (Dobro et al., 2010). All of them, however, rely on using macroscopically large filter paper surfaces to blot the sample to a thin film on the order of 100's of nm in depth. The outcome of this method is often not optimal, with large areas of the grid surface covered in vitrified sample that is either too thick or too thin and thus unsuitable for particle imaging. Even highly skilled technicians may need to spend considerable effort optimizing this process for a new specimen; precious specimen is consumed by each trial, and time is wasted both in the laboratory and on the microscope to evaluate the prepared grids. Specimen preparation thus remains a bottleneck for the field of cryo-TEM and new techniques are needed to provide vitrified samples in a more controlled and efficient manner.

In addition to the traditional method of specimen pipetting and blotting, a variant method involves creating a dense spray of specimen (1–20 μm droplets) using nebulizers, micro-nozzles and electrospray mechanisms (Berriman and Unwin, 1994; White et al., 2003; Lu et al., 2009), where the grid is plunged through the

* Corresponding author. Fax: +1 858 784 9090.
E-mail address: tjain@scripps.edu (T. Jain).

1047-8477/$ - see front matter © 2012 Elsevier Inc. All rights reserved.
http://dx.doi.org/10.1016/j.jsb.2012.04.020

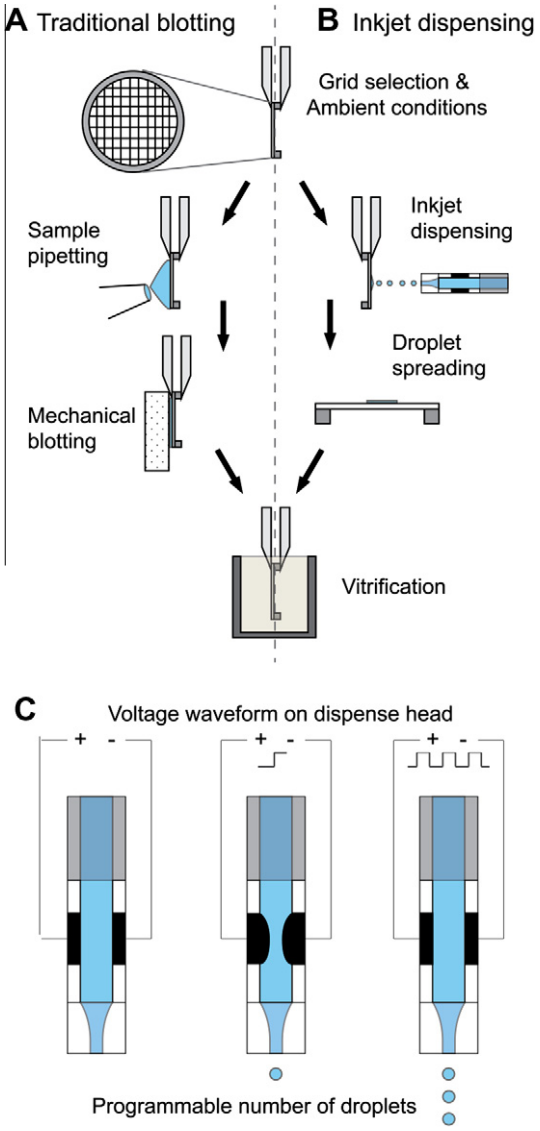

Fig.1. Traditional blotting vs. new method for vitrification of specimens. (A) Traditional method comprised of pipetting specimens (~3 μL) onto TEM grids, followed by manual blotting and plunge into liquid ethane. (B) New method utilizes inkjet dispensing of picoliter to nanoliter volumes of specimens onto grids, surface spreading of droplets followed by vitrification. (C) Inkjet head based on piezo-electric technology enables programmable specimen dispensing in discrete droplets utilizing accurately timed voltage pulses.

sprayed region on its way to vitrification in the liquid ethane bath. Droplets landing on the grid surface spread out on contact due to surface hydrophilicity and do not need further blotting. A major advantage of this method is the precise timing and in-flight application of the specimen to the grid, which allows for rapid (sub-10 ms) molecular events to be trapped, thus allowing for time-resolved cryo-TEM studies (Walker et al., 1999; Barnard, 2009; Lu et al., 2009). While this method does not use blotting, there is little control over individual droplet sizes or the precise timing of when the droplets impact the grid surface. Obtaining ice of suitable thickness due to droplet spreading thus remains an unpredictable process dependent on the individual droplet behavior and its interaction with the grid. Moreover, the liquid-handling devices used for these processes often entail large dead-volumes and thus specimen wastage, perhaps one of the primary reasons why this particular method has not seen more mainstream usage.

New technology for dispensing precisely controlled volumes of sample onto discrete spots on a surface has been driven by the interest and investment in DNA and protein microarrays; recently using non-contact "print-heads" to spot biological samples onto precisely defined targets on a microscope slide (Jain et al., 2012). Non-contact printing can be achieved using piezoelectric "inkjet" printing (Kyser et al., 1981), a technology developed over the last 30 years. The technique uses a piezoelectric element to impulsively impart an acoustic pressure wave to liquid in the tip of a fine nozzle, causing a droplet of the liquid to be ejected from the tip, precisely controlled to 10's of pL (Wijshoff, 2010). Additionally, and of particular interest to cryo-TEM, is that piezo-electric based dispensing is compatible with a wide range of biological specimens such as nucleic acids (Blanchard et al., 1996), proteins (Nagaraj et al., 2008; Nagaraj, 2011), bacteria (Bruns et al., 2003), mammalian cells (Saunders et al., 2008) and nanoparticles, micron-sized beads, polymers and aggregates (for a detailed review refer to (Calvert, 2001)). Moreover, inkjet print-heads are available commercially and are robust due to the technological maturity of the microarray market. Given these technical and logistical advantages, we have initiated the integration of piezo-electric inkjet technology as a specimen application step in cryo-TEM to increase the efficiency of obtaining thin vitrified particles (Fig. 1B).

In this paper, we describe a prototype that integrates a piezo-electric inkjet dispense head into a custom-designed vitrification system. Picoliter to nanoliter volumes of specimens were dispensed onto continuous and holey carbon grids, plunge-vitrified and evaluated by particle imaging using cryo-TEM. Precise volumes were programmed by selecting the total number of discrete droplets (32 pL each) ejected from the inkjet head using a rectangular pulse train (Fig. 1C). The droplets are monitored in real-time using side and rear view cameras to study the in-flight and on-grid droplet dynamics, respectively. Results indicate the feasibility of obtaining thin-ice areas suitable for particle imaging. Real-time imaging using the rear-view camera system provides detailed information regarding the spreading and evaporation profiles for various droplet-substrate configurations; useful to study the droplet dynamics and determine critical time points. While piezo-electric inkjet dispensing has been utilized for fabricating protein arrays, to our knowledge there is no report of its use in TEM specimen preparation. Therefore, a concern regarding particle stability post-dispensing was addressed to ensure that the electro-physical mechanism of piezo-electric dispensing itself did not disrupt macromolecular structure or degrade proteins (using specimens such as Tobacco Mosaic Virus, GroEL, Lipid Nanotubes, Microtubules and Cucumber Necrosis Virus).

The developments reported here provide strong evidence of the feasibility of using inkjet technology (in this case based on piezo-electric dispensing) as an improved method for delivering specimen onto grids prior to vitrification. As this is a first prototype system, controls for a variety of critical environmental parameters (e.g. relative humidity, temperature) have not yet been incorporated. Also, droplet spreading was limited by the surface wettability of carbon films achievable by traditional plasma treatments and thin ice reported here was obtainable only after significant evaporation. Work in progress now includes incorporating these environmental controls and substantially increasing surface wettability to maximize droplet spreading and minimize the need for evaporation.

2. Materials and methods

2.1. Equipment setup

The instrument is constructed on a vibration resistant breadboard (Performance Series I, ThorLabs, CA), as shown in Fig. 2A–C

and S3, and comprises of four major subsystems: (i) An inkjet dispensing system, (ii) A pneumatic plunging system, (iii) A side-view camera system, and (iv) A rear-view camera system. The inkjet dispensing system consists of a 24 μm bore piezo-electric inkjet dispense head (Engineering Arts, AZ) hydraulically coupled to a syringe pump via control valves and finally to a 0.2 μm filtered water reservoir. Prior to sample aspiration and inkjet dispensing, the water column is flushed with 500 μL of water to remove any residual particles or bubbles, and to establish a continuous water column between the dispense head tip and water reservoir. Thereafter, the piezo-electric inkjet controller (DE03, Engineering Arts, AZ) triggers a sequence of programmable rectangular pulses corresponding to single droplet generation. Droplet generation is verified by the side-view camera system (described below) and in case of inconsistent droplet profiles, the inkjet head is flushed again as described above. Thereafter, the sample is aspirated (~5 μL) and similarly verified for droplet generation using the side-view camera. The inkjet head is mounted onto a miniature pneumatic slide table (MXQ6-20, SMC Corp., IN), allowing for switching between two (20 mm separated) positions using a (first) lever controlled manual pneumatic valve. The dispense head/pneumatic slide table assembly is further mounted onto a manual rotation and three-axis stage (Newport, CA) for precise positioning of the inkjet head relative to the EM grid. The pneumatic plunging system is comprised of a manual toggle clamp mounted to the external rod of a pneumatic plunge cylinder (MTS20-100-F9BL, SMC Corp., IN). The toggle clamp holds a fine tipped tweezers, which is used to hold the EM grid. The mounting panel of the pneumatic plunge cylinder is attached to a three-axis manual stage (Model A, Line Tools, PA) mounted on a raised solid aluminum platform. Plunge of the pneumatic cylinder into a reservoir of liquid ethane placed directly below is initiated using a (second) lever controlled manual pneumatic valve. The side-view camera system consists of a monochromatic camera (UEYE UI-1220SE-M, IDS Imaging, MA) illuminated by an LED strobe-light. The strobe-on pulses are generated by the piezo-electric controller at a delay and time-period post-dispensing single droplets (typically 10 and 100 μs, respectively). The rear-view camera system is comprised of an objective lens turret holding a 4X, 10X and 20X objective lens (OT1, RMS4X, RMS10X, RMS20X – Thorlabs, CA), and connected to a 30 mm cage cube with a dichroic filter via lens tubes (C4 W, MD499, SM1L – Thorlabs, CA). A blue LED controlled by an LED driver (M470L2, LEDD1B Thorlabs, CA) supplies the inlet light source. A rear-view camera (DVC340 M, DVC Company, TX) is attached to the cube for real-time image capture and image acquisition controlled by a custom application written in Java (utilizing the camera API supplied by the vendor).

2.2. Precise spatial targeting and fluorescence imaging of inkjet dispensed specimens

A fluorescence dye (Atto 488, Atto-Tec GmbH, Germany) was diluted to 1 μg/mL in Phosphate Buffered Saline and aspirated into the inkjet dispense head and verified for droplet generation as

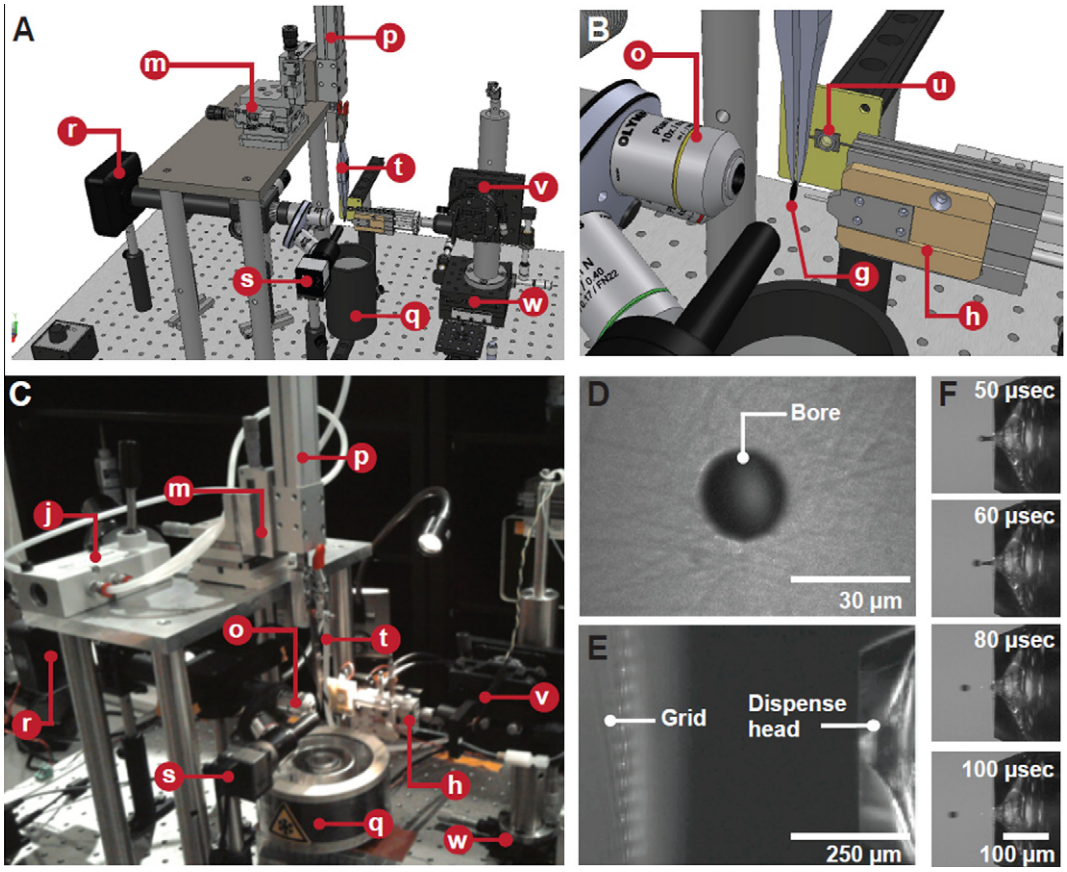

Fig.2. Equipment model, setup and inkjet head positioning. (A) 3D model of equipment components (notations provided below), comprised of the plunge axis, rear and side-view optics, dispense head and positioning stages. (B) Close-up model view of the inkjet dispense head positioned in proximity to the EM grid and the specimen dispense process monitored by the rear and side-view optics. (C) Integrated equipment setup for inkjet dispense and vitrification (notations provided below). (D) Front view of the inkjet dispense head utilized for picoliter to nanoliter specimen dispensing. (E) Side view showing the positioned EM grid and inkjet dispense head prior to specimen dispense. (F) Time-lapse sequence of a single droplet of specimen (~32 pL) dispensed from the inkjet head. Notations in (A–C): (g)–EM grid, (h)–inkjet dispense head mounted on pneumatic stage, (j)-manual pneumatic plunging valve, (m)-manual 3-axis positioner holding plunge assembly, (o)-rear-view objective lens, (p)-pneumatic plunge assembly, (q)-liquid ethane reservoir, (r)-rear-view camera, (s)-side-view camera, (t)-tweezers holding EM grid, (u)-LED strobe light, (v)-manual rotation and z-axis stage and (w)-manual 2-axis stage for positioning dispense head.

described above. Droplet positioning relative to the rear-view camera was performed using a plain glass slide mounted on the plunge assembly (instead of the tweezers). The three axis stage carrying the inkjet dispense system was positioned to obtain a droplet at the center of the camera field of view. Thereafter, a holey carbon grid (CFlat 2 μm holes, 0.5 μm spacing – ProtoChips Inc., NC) was treated (or not) in an Oxygen/Argon plasma environment (Solarus Model 950, Gatan Inc., CA) for 5–10 s and positioned in front of the objective using tweezers mounted on the plunge assembly. The targeted square areas of the grid were manually aligned using the three-axis stage to the center of the field of view of the rear-view camera and at ~500 μm from the tip of the inkjet dispense tip (Fig. 2D). Thereafter, 64 pL (2 droplets) were dispensed into the targeted squares and the grid repositioned to create the desired pattern. The grid was subsequently imaged on an inverted fluorescence microscope (TE-2000U, Nikon, USA).

2.3. Structure and biochemical assay of macromolecules post-inkjet dispensing

Macromolecules in their compatible buffers including GroEL, Ni-Lipid Nanotubes, Microtubules and Cucumber Necrosis Virus (CNV) were aspirated and dispensed (32 nL) onto continuous carbon grids (previously treated with plasma, as described above). Shortly after dispensing, the dispense head was retracted, and 3 μL of 2% Uranyl Acetate was manually pipetted onto the grid and blotted away with filter paper (Grade I, Whatman-GE Healthcare). After drying, these negatively stained grids were imaged using a Technai Spirit TEM (FEI Inc., OR) at various magnifications (500–50,000×). Biochemical assays for stability of functional activity of macromolecular complex Human Dicer/TRBP was conducted pre- and post-inkjet dispensing. The Dicer–TRBP complex was purified as previously described (Lau et al., 2009). The sample was divided into two fractions of 7 μL; one was passed through the inkjet dispenser while the other was kept as control. Both samples were used in an assay verifying dicing activity (MacRae et al., 2007). Briefly, dicing reactions were carried out at 37 °C and contained 50 mM NaCl, 3 mM MgCl2, 20 mM Tris (pH 7.5). A Cy5-labeled dsRNA, 30 base-pair long, was used as the substrate to test the dicing ability of the complex into identifiable ~21–22 nucleotide fragments. The dsRNA was then incubated with the Dicer/TRBP enzyme complex (at 400 nM) samples from the experimental and control vials for 15-min and 45-min time points. Thereafter, the reagents were run on a 14% PAGE gel and the gel imaged to identify the product band.

2.4. Vitrification protocol

Specimens were diluted in appropriate buffers and concentrations (GroEL: 100 μg/mL; Tobacco Mosaic Virus – TMV: 100 μg/mL) and pipetted into a sample vial for aspiration. The inkjet dispense head was flushed with water and verified for droplet generation as described above. Thereafter, 5 μL of specimen was aspirated from the sample reservoir and droplet generation confirmed using the side-view camera. A plasma-treated continuous carbon grid (prepared in house) or holey carbon grid (Protochips, Inc.) were held with fine tweezers and mounted in position on the pneumatic plunge system. A liquid ethane reservoir (surrounded by liquid nitrogen) was prepared and positioned below the plunge assembly. Thereafter, a precise amount of specimen was dispensed, the pneumatic slide table (holding the inkjet head) retracted and the grid plunged into liquid ethane, all under manual control. Throughout the process the rear-view camera provided real-time visual feedback on the monitor and recorded 100 Hz frame rate video into computer memory. The vitrified grids were rapidly transferred into liquid nitrogen, as per standard cryo-TEM protocol (Grassucci et al., 2007), and stored in liquid nitrogen dewars until cryo-TEM imaging.

2.5. Cryo-TEM imaging

Vitrified grids as described above were transferred under liquid nitrogen into a cryo-cooled grid holder, as per standard cryo-TEM protocol (Grassucci et al., 2007). The grid holder was then inserted into a Technai F20 or Spirit TEM microscope (FEI Inc., OR). The Leginon system was used for all automated microscopy and image capture (Suloway et al., 2005). Initially, the specimen was manually located on the grid at the targeted regions. Thereafter, a low magnification (~100x) atlas was generated and a mosaic generated surrounding the specimen region. Medium (500–5000x) and high-magnification images (50,000x) were acquired using the Leginon multi-scale imaging application (Suloway et al., 2005).

3. Results

3.1. Piezo-electric inkjet dispensing and vitrification system

To test if picoliter to nanoliter dispensing of specimen using piezo-electric inkjet technology can be utilized for cryo-TEM, we developed a custom system that integrated several modules as shown in Fig. 2A–C. A commercially available piezo-electric dispense head was incorporated with central bore size 24 μm (Fig. 2D). This head was capable of dispensing discrete specimen droplets of 32 pL; observed in-flight using a stroboscopic LED light and side-view lens/camera system, which allowed for viewing dispensed droplets at precise time-points (0–100 μsecs) after droplet generation from the head (Fig. 2F and for video see S.1). Specimen dispense was triggered by software via the accompanying piezo-electric head control module and the number of droplets, frequency and droplet velocity could be modified as desired. S.2 shows a video of 1000 droplets (32 nL), being dispensed onto a continuous carbon EM grid located 500 μm from the dispense head (Fig. 2E), demonstrating on-axis and linear trajectory of dispensed droplets. Rear-view imaging at an acquisition rate of 100 Hz allowed for visualizing droplet impact, spreading and evaporation dynamics. The rear-view camera was also used to align the grid with the dispense head and provided a way to visualize different dispense conditions on the same grid (prior to vitrification). The grid and dispense head were independently manipulated for alignment using two 3-axis manual positioners, which allowed for precise targeting of specimen droplets on the grid. The close proximity of the dispense head to the grid (500 μm) required retracting the head away immediately after the dispense sequence was completed (in order to protect it from being damaged by the tweezers holding the grid), prior to initiating the plunge into liquid ethane. This was accomplished by mounting the dispense head on a miniature pneumatic stage whose binary position (in or out) was controlled by a hand-operated pneumatic valve. A 90° rotation stage was incorporated to rotate the dispense head between the vertical (specimen aspiration) and horizontal (specimen dispense) positions, which also provided a way to retrieve remaining specimen from the dispense head. The vertical position allowed for specimens to be aspirated directly from vials and well-plates. The overall sequence of events from specimen aspiration into the head, to droplet dispense onto a grid and plunge into liquid ethane is shown in an animated solid model (video S.3).

3.2. Spatial targeting and influence of substrate hydrophilicity on droplet spreading

We next evaluated the feasibility to spatially dispense specimen droplets to targeted areas on the grid. The ability to precisely align

and confine droplets on the substrate could open up the possibility for delivery of multiple samples per grid in the future, increasing the throughput of cryo-TEM experimentation. The inkjet head was used to dispense droplets into targeted grid squares to write the letters "N", "R", "A" and "M" using 64 pL (2 droplets) per grid-square (Fig. 3A), aligned using the 3-axis manual micro-positioner. The positioning was possible by first registering the droplet (on sacrificial areas), and then moving subsequent targeted areas of the grid to the center using the rear-view camera. Spatial targeting was confirmed by fluorescence imaging of the specimens (ex/em: 488/520 dye) on the grid. Droplet impact and spreading was further studied in hydrophobic and hydrophilic conditions. As shown in Fig. 3B, for untreated carbon grids the contact angle observed was ~90°, upon droplet dispensing (25 droplets) and image capture. In contrast, as shown in Fig. 3C, when the carbon grids were treated in an Oxygen/Argon plasma discharge, the contact angles reduced to ~15°. This effect of surface wettability was evaluated for smaller volume (64 pL, 2 droplets) dispensing of fluorescent specimens on holey carbon grids by fluorescence and phase imaging (Fig. 3D–E), with marked improvement in droplet spreading and uniformity within the targeted squares for the hydrophilic conditions.

3.3. Real-time visualization of droplet dynamics on EM grids

As one of the goals of this new methodology is to eliminate manual blotting, it is important that the grid be vitrified at time-points when the sample thickness is suitable for cryo-TEM imaging. This can be accomplished by viewing the droplet dynamics (spreading and drying) on the grid in real-time and triggering the plunge process (for vitrification) at an optimal time-point post-dispensing. Fig. 3F shows specific frames of a time-series (0–300 ms) of 1 droplet (32 pL) targeted within a square of a holey carbon grid (S.4 for a 100 Hz frame rate video). At the existing environment conditions (RH 10%, Temperature 25 °C), a single droplet dries (as observable by rear-view imaging) within 300 ms upon impact onto the grid. Fig. 3G shows mean drying times observed for multiple droplets (1 to 10) at similar environmental conditions. Under these conditions, higher number of droplets led to longer drying times (and also larger spreading distances on the grid; data not shown). Also, the repeatability of the droplet dynamics (based on drying times) is high for the droplets dispensed on the grid, allowing for automated plunging events to be accurately timed in future systems.

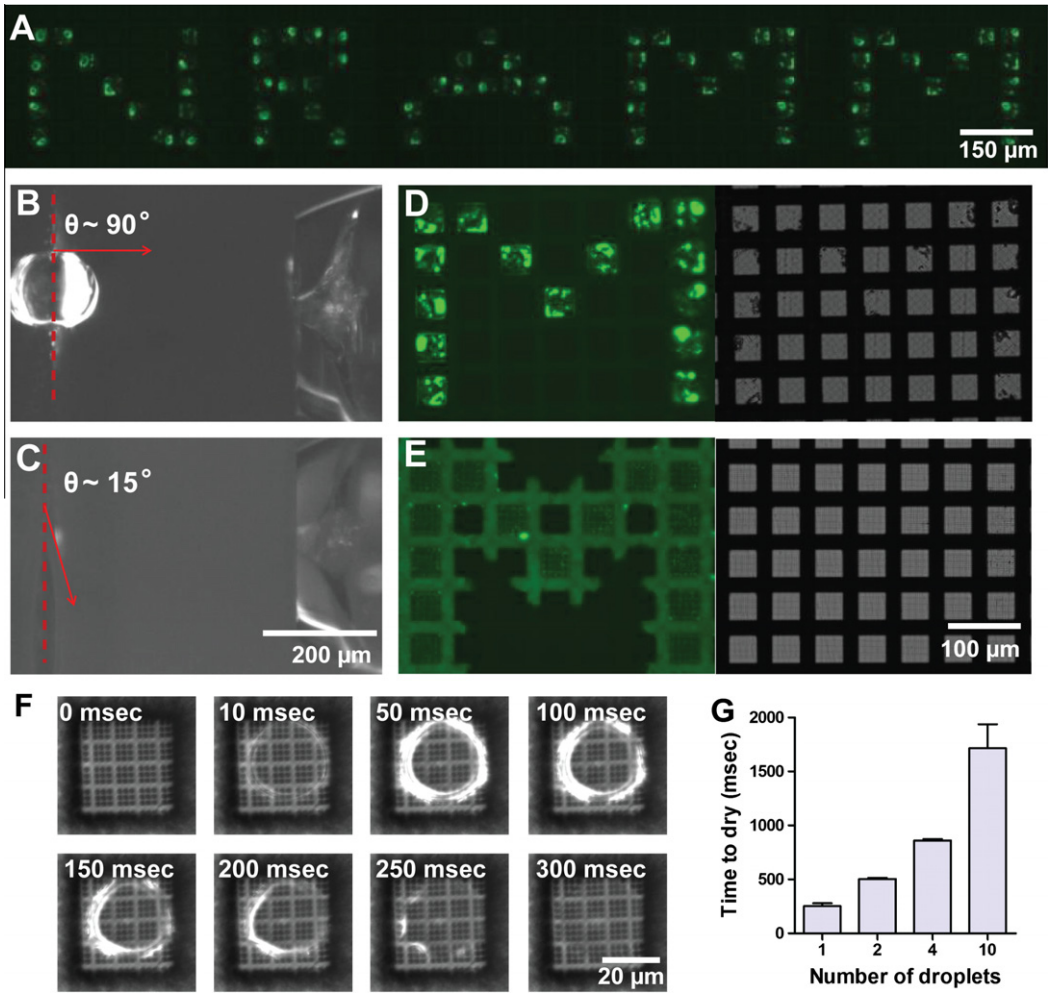

Fig.3. Precise spatial and temporal control of specimen dispensing on EM grids. (A) Fluorescent light microscopy images of the letters "N", "R", "A" and "M" printed on a single EM grid using inkjet dispensing of 64 pL (2 droplets) fluorescent dye into individual square targets (~30 µm) using manual positioning. (B–C) Side-view image of 8 nL dispensed (25 droplets) on (B) untreated and (C) plasma treated continuous carbon EM grids with corresponding contact angles. (D–E) Fluorescent and phase light microscopy of inkjet dispensed specimens on (D) untreated and (E) plasma treated holey carbon grids indicating non-uniform and uniform spreading, respectively. (F) Spatial targeting of a single droplet (32 pL) within a square of a holey carbon grid and real-time image sequence capture using the rear-view camera. (G) Graph indicating mean drying times of 1–10 droplets of specimens dispensed onto EM grids as evaluated by real-time rear-view imaging (under environmental conditions RH: 10% and Temp: 25 °C).

3.4. Particle structure and functional stability

For application of inkjet technology to TEM imaging, it is imperative that the dispensing technology itself does not degrade the macromolecules or their complexes. Therefore, to evaluate the effect of the piezo-electric inkjet heads on particle structure stability, several macromolecules with known structures (GroEL, Microtubules, Lipid Nanotubes, Cucumber Necrosis Virus) were dispensed (32 nL, 1000 droplets) onto carbon-film grids and then subsequently negative stained manually with 2% Uranyl Acetate (negative stain applied within 10 s of sample dispensing). As shown in Fig. 4A–D, particles in all four cases were structurally intact (comparable to their previously known structures) with no evidence of morphological disruption. To further confirm the compatibility of piezo-electric inkjet dispensing for maintaining functional activity of eukaryotic complexes, human Dicer/TRBP complex was dispensed via the piezo-electric inkjet head into a test aliquot and its ability to dice double stranded RNA compared to control aliquots. Results indicated that the inkjet dispensing did not affect the dicing activity (incubation time-periods of 15 and 45 min) of the Dicer/TRBP complex as assessed on an RNA gel (Fig. S.7).

3.5. Inkjet specimen dispensing, vitrification and cryo-TEM

Following confirmation that biological macromolecules appeared stable after inkjet dispensing and that droplet dynamics were observable in real-time on the grid, the next step was to establish feasibility of using the integrated inkjet dispensing, plunging and vitrification system to obtain samples suitable for cryo-TEM imaging. For this purpose, 1.6 nL (50 droplets) of Tobacco Mosaic Virus (TMV) and 3.2 nL (100 droplets) of a molecular chaperone (GroEL), were dispensed onto continuous carbon (Fig. 5A) and holey carbon grids (Fig. 5B) respectively, and vitrified at time-points prior to complete drying of the droplet. All experimental conditions were at RH 10% and temperature 25 °C, with the plunge process triggered under manual operator control (using real-time visual feedback from the rear-view camera). The continuous carbon grids provided a non-porous surface for droplet spreading, which allowed for uniform spreading in a radial manner (video S.5). Also, after the spreading was complete (within 200 ms) and the droplet was pinned, drying patterns could be observed within 2 s (Fig. 5A, top row). On visual onset of the drying patterns, the grids were plunged for vitrification and imaged using cryo-TEM. At low magnification, typical spot profiles were circular with dark (thicker) center areas and lighter (thinner) areas towards the perimeter. Droplet thickness was such that TMV particles could be observed only in the peripheral areas (Fig. 5A, bottom row). In the case of holey carbon grids (porous due to the 2 μm holes), the spreading profile was more complex. Instead of uniform circular spreading, the dispensed volume traversed through the 2 μm holes in the carbon membrane to both sides of the grid, spreading and then contacting the support copper mesh, which induced local droplet dynamics within the squares (video S6). Sample spreading over the grid is complete within 300 ms and the manual plunge triggered at 4 s, when the sample was observed receding due to evaporation (Fig. 5B, top row). Low-magnification cryo-TEM images correlate with observations on the 100 Hz real-time videos, indicating individual squares displaying local droplet drying dynamics (Fig. 5B, bottom row). Squares on the grid could be identified where vitrified sample was thin enough for visualizing GroEL in vitrified ice suspended over holes. For TMV particles, the 23 A° diffraction patterns were identifiable, and for GroEL, two-dimensional class averages of selected top-view particles indicated sevenfold symmetry – both results suggesting preservation of particle morphology.

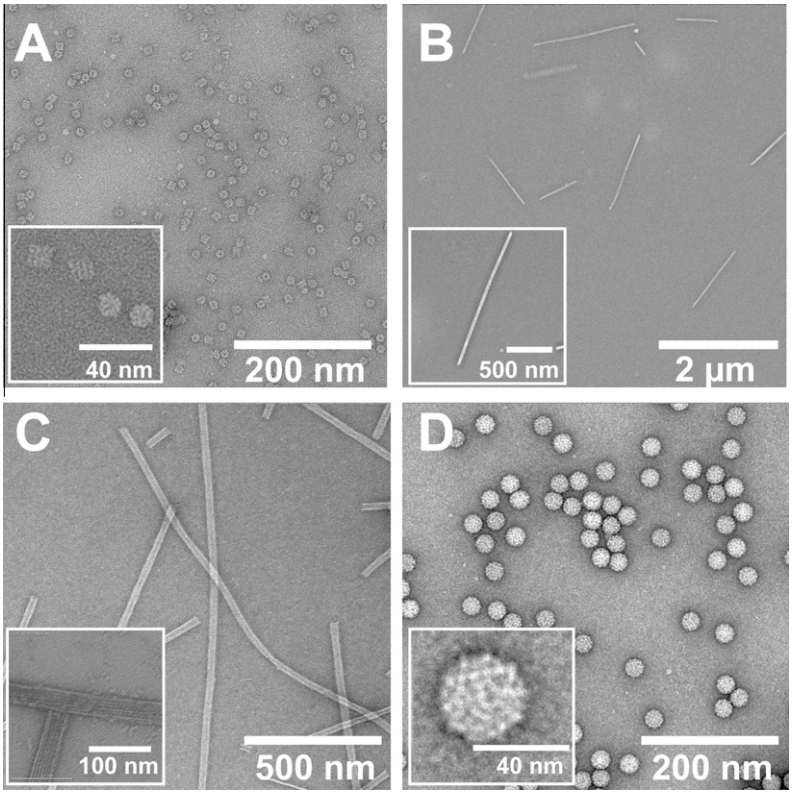

Fig.4. Structural and functional preservation of macromolecules dispensed using the piezo-electric inkjet head. Negative stains of inkjet dispensed macromolecules including (A) GroEL, (B) Ni-Lipid Nanotubes, (C) Microtubules and (D) Cucumber Necrosis Virus (CNV) particles. Insets show magnified views of each macromolecule.

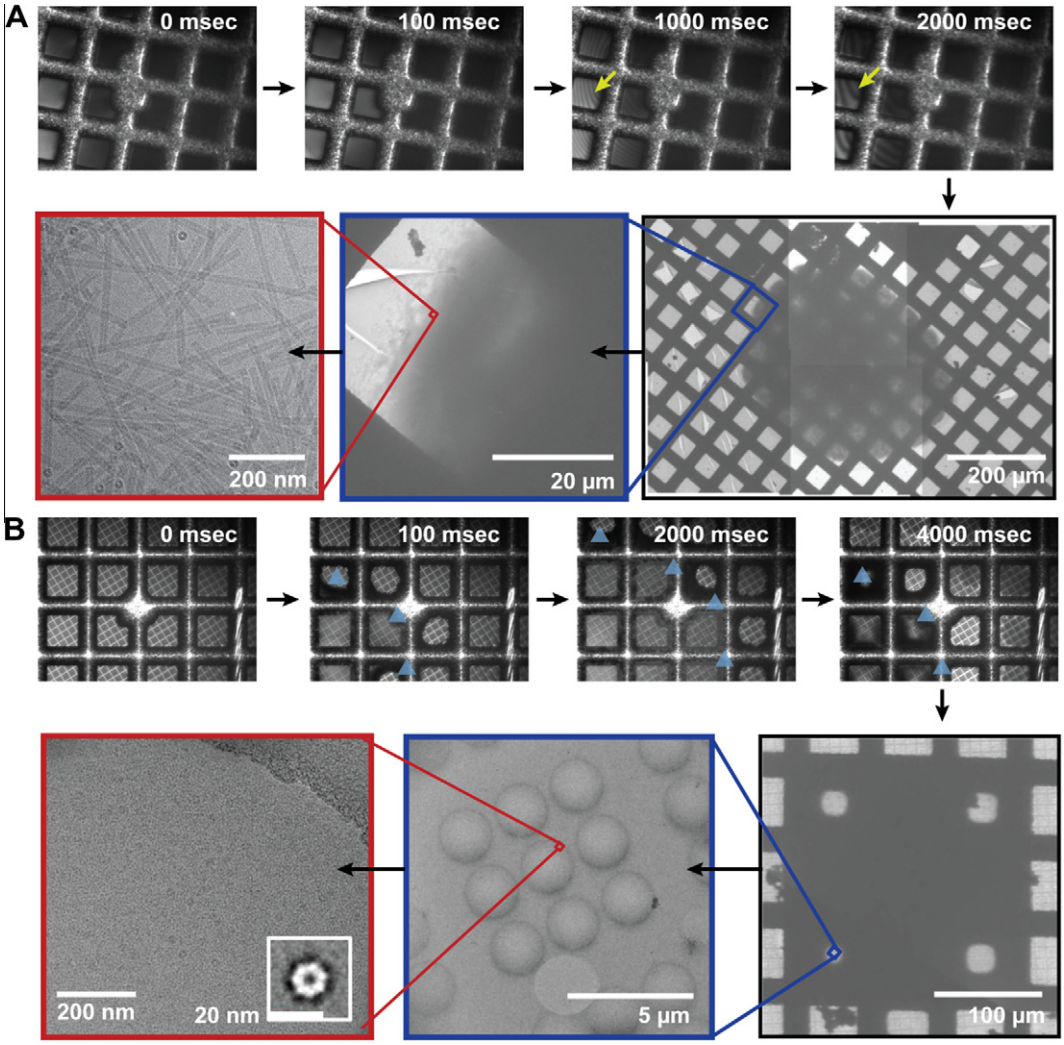

Fig.5. Inkjet dispensing, vitrification and cryo-TEM of specimens on EM grids. (A) Top panel: Inkjet dispense and vitrification of 1.6 nL (50 droplets) of Tobacco Mosaic Virus (TMV) onto continuous carbon grids and rear-view imaging of specimen drying profiles. Yellow arrows indicate onset of drying within specific regions and after specified time-points. Bottom panel: Cryo-TEM imaging of specimen prepared above at low (100×), medium (560×) and high magnification (52,000×). (B) Top panel: Inkjet dispense and vitrification of 3.2 nL (100 droplets) of GroEL onto holey carbon grids and rear-time imaging of specimen drying profiles. Blue arrows indicate edge profile of dispensed sample on the grid after specific time-points. Bottom panel: Cryo-TEM imaging of specimen prepared above at low (120×), medium (5000×) and high magnification (50,000×). Inset represents a 2D class average of GroEL particles.

4. Discussion and conclusion

As investigated in this study, integration of inkjet dispensing and plunge vitrification for cryo-TEM sample preparation offers several advantages. Primarily, the volume of specimen used is greatly reduced compared to traditional pipetting and manual blotting techniques (~3 μL specimen volume), by a factor of at least 1000x (~3 nL, 100 droplets dispensed). With further optimization, substrate and instrument development (discussed below), specimen usage could be further reduced to 100,000× (~32 pL, single droplet dispensed). Such reduction in required specimen volume will be particularly valuable in cases of limited availability (such as eukaryotic membrane proteins and complexes) where optimizing sample preparation conditions is a major bottle-neck for cryo-TEM imaging. Given the repeatability of inkjet dispensing and droplet dynamics (exemplified in Fig. 3E–G), research groups should be able to archive accurate dispense parameters that yielded optimal vitrification for a particular specimen, resulting in improved success for cryo-TEM imaging and particle reconstruction.

Inkjet dispensing using the piezo-electric heads in this study, maintained specimen stability as evaluated by imaging the structure and function of known macromolecules post-dispensing on carbon grids or by biochemical assay (Fig. 4A–D, Fig. S.7 and 5A and B), which supports the potential of this novel method for cryo-TEM sample preparation. In the current instrument (Spotiton v0.5), a rear-view camera (with accompanying optics) was positioned behind the grid (Fig. 2A–B). This enabled a number of novel features, including the ability to spatially target the specimen droplets precisely on desired locations on the grid (Fig. 3A–E) and real-time visualization of droplet dynamics on-grid for evaluating spreading and drying profiles (Fig. 3F and G). Specimens were targeted to the center of the grid (physically marked and optically identifiable), which enabled rapid identification of the dispensed spot during TEM low magnification imaging (Fig. 5A and B). Future versions of the instrument will take advantage of this precise spatial targeting and potentially also include multiple dispense heads to enable multiple specimen dispensing on a single grid. This is expected to significantly increase sample preparation throughput and cryo-TEM imaging, to ~10 samples on a single grid (3 mm diameter standard) with sufficient area coverage for each spot for TEM imaging and particle reconstruction.

While piezo-electric inkjet technology offers several advantages, much development is required to mature this technology into

a mainstream technique for cryo-TEM sample preparation. In the current instrument (Spotiton v0.5), pneumatic stages were used under manually operated valves to trigger the plunge process, which limited the accurate control of these time-periods. Also, the environment relative humidity (room at RH 10%) and temperature (25 °C) were not controlled to limit evaporation prior to vitrification. This is not ideal given that protein specimens can often be sensitive to concentration changes (increasing salts, buffers and inter-molecular interactions) due to evaporation. In future instrument versions, light-weight high-speed motors and encoders will be utilized to accurately trigger the plunge process and time to vitrification. Also, an environment chamber will be incorporated to control the relative humidity and temperature to minimize evaporation.

Even if the timing parameters and environmental conditions are accurately controlled, a necessary requirement for generating samples suitable for cryo-TEM imaging is to vitrify the specimens within a few hundred nanometers of thickness, for optimal imaging conditions. However, even for reduced contact angles measured at ~15°, inkjet dispensing and vitrification led to large surface areas of thick ice unsuitable for cryo-TEM imaging (Fig. 5A and B). Only the areas at the edge of the droplet lend themselves to particle imaging. Thus, while these results provide initial proof that inkjet dispensing and vitrification can be used for cryo-TEM sample preparation and particle imaging, the current method is clearly not optimal. For surfaces traditionally considered hydrophilic (water contact angles 10°–15°), the estimated initial central height (prior to the evaporation stage) for single droplets (~32 pL) on hydrophilic surfaces is within the 5–10 μm range, unsuitable for cryo-TEM imaging. We therefore envision the need to further increase the surface hydrophilicity down to contact angles close to 0° to achieve large areas of vitrified samples with the desired thickness (~100's nm, Supplementary S.8). It has been demonstrated that 'super-hydrophilic' substrates (having contact angles close to 0°) can be achieved by a variety of surface chemical, material deposition and physical methods (Feng and Jiang, 2006). Realizing such 'super-hydrophilic' states on EM grids is currently under study and is expected to result in larger droplet spread (more imaging surface area) and thinner vitrified samples suitable for cryo-TEM imaging.

In conclusion, inkjet dispensing of picoliter to nanoliter volumes of specimen integrated with grid plunging and vitrification provides a novel methodology for cryo-TEM sample preparation. Towards this goal, a first prototype instrument (Spotiton v0.5) was developed and preliminary experiments conducted to evaluate the compatibility of inkjet heads (in this case piezo-electric based) for macromolecule specimen dispense onto carbon film EM grids (continuous and holey) with subsequent vitrification and cryo-TEM imaging.

Acknowledgments

We thank Elizabeth Wilson for kindly donating Ni-Nanotube and microtubule samples, Tom Smith for the CNV samples, Rueben Diaz for TMV samples, Eli Chapman for GroEL samples and Pick-Wei Lau for the Dicer/TRBP complex and dicing activity assays. Peter Kahn and Peter Wiktor from Engineering Arts LLC (Tempe, AZ) for their invaluable discussion and initial training with the DE03 inkjet dispense unit. Steven B. Bradlow for modeling the geometry and calculations pertaining to the droplet profile. This work is supported by grants from the National Center for Research Resources (RR017573) and the National Institute of General Medical Sciences (GM103310) from the National Institutes of Health.

Appendix A. Supplementary data

Supplementary data associated with this article can be found, in the online version, at http://dx.doi.org/10.1016/j.jsb.2012.04.020.

References

Barnard, D., Lu, Z., et al., 2009. "Time resolved cryo-electron microscopy of ribosome assembly using microfluidic mixing". Microscopy and Microanalysis 15 (Suppl. S2), 942–943.
Berriman, J., Unwin, N., 1994. Analysis of transient structures by cryo-microscopy combined with rapid mixing of spray droplets. Ultramicroscopy 56 (4), 241–252.
Blanchard, A.P., Kaiser, R.J., et al., 1996. High-density oligonucleotide arrays. Biosensors & Bioelectronics 11 (6–7), 687–690.
Bruns, A., Hoffelner, H., et al., 2003. A novel approach for high throughput cultivation assays and the isolation of planktonic bacteria. Fems Microbiology Ecology 45 (2), 161–171.
Calvert, P., 2001. Inkjet printing for materials and devices. Chemistry of Materials 13 (10), 3299–3305.
Dobro, M.J., Melanson, L.A., et al., 2010. Plunge freezing for electron cryomicroscopy. Methods in Enzymology 481, 63–82.
Dubochet, J., McDowall, A.W., 1981. "Vitrification of pure water for electron microscopy. Journal of Microscopy 124 (3), 3–4.
Feng, X.J., Jiang, L., 2006. Design and creation of superwetting/antiwetting surfaces. Advanced Materials 18 (23), 3063–3078.
Grassucci, R.A., Taylor, D.J., et al., 2007. Preparation of macromolecular complexes for cryo-electron microscopy. Nature Protocols 2 (12), 3239–3246.
Jain, T., Papas, A., et al., 2012. In situ electroporation of surface-bound siRNAs in microwell arrays. Lab on a Chip 12 (5), 939–947.
Jensen, G.J., 2010a. "Cryo-EM, Part A: sample preparation and data collection. Preface". Methods in Enzymology 481, xv–xvi.
Jensen, G.J., 2010b. "Cryo-EM, Part B: 3-D reconstruction Preface". Methods in Enzymology 482, xv–xvi.
Jensen, G.J., 2010c. Cryo-EM, Part C: analysis preface. In: Grant, J.J. (Ed.), Methods in Enzymology. Academic Press, vol. 483, pp. v–xvi.
Kyser, E.L., Collins, L.F., et al., 1981. Design of an impulse ink jet. Journal of Applied Photographic Engineering 7 (3), 73–79.
Lau, P.W., Potter, C.S., et al., 2009. Structure of the human Dicer-TRBP complex by electron microscopy. Structure 17 (10), 1326–1332.
Lepault, J., Booy, F.P., et al., 1983. Electron microscopy of frozen biological suspensions. Journal of Microscopy 129 (1), 89–102.
Lu, Z., Shaikh, T.R., et al., 2009. Monolithic microfluidic mixing-spraying devices for time-resolved cryo-electron microscopy. Journal of Structural Biology 168 (3), 388–395.
MacRae, I.J., Zhou, K., et al., 2007. Structural determinants of RNA recognition and cleavage by Dicer. Nature Structural & Molecular Biology 14 (10), 934–940.
Nagaraj, V.J., Eaton, S., et al., 2008. Piezoelectric printing and probing of Lectin NanoProbeArrays for glycosylation analysis. Biochemical and Biophysical Research Communications 375 (4), 526–530.
Nagaraj, V.J., Eaton, S., et al., 2011. NanoProbeArrays for the Analysis of Ultra-Low-Volume protein samples using piezoelectric liquid dispensing technology. Journal of Laboratory Automation 16 (2), 126–133.
Saunders, R.E., Gough, J.E., et al., 2008. Delivery of human fibroblast cells by piezoelectric drop-on-demand inkjet printing. Biomaterials 29 (2), 193–203.
Suloway, C., Pulokas, J., et al., 2005. Automated molecular microscopy: the new Leginon system. Journal of Structural Biology 151 (1), 41–60.
Walker, M., Zhang, X.Z., et al., 1999. Observation of transient disorder during myosin subfragment-1 binding to actin by stopped-flow fluorescence and millisecond time resolution electron cryomicroscopy: evidence that the start of the crossbridge power stroke in muscle has variable geometry. Proceedings of the National Academy of Sciences of the United States of America 96 (2), 465–470.
White, H.D., Thirumurugan, K., et al., 2003. A second generation apparatus for time-resolved electron cryo-microscopy using stepper motors and electrospray. Journal of Structural Biology 144 (1–2), 246–252.
Wijshoff, H., 2010. The dynamics of the piezo inkjet printhead operation. Physics Reports-Review Section of Physics Letters 491 (4–5), 77–177.